ASIAN JOURNAL OF CIVIL ENGINEERING (BHRC) VOL. 16, NO. 3 (2015)
PAGES 417-436

SEISMIC BEHAVIOR OF BENCHMARK BUILDING WITH SEMI-ACTIVE VARIABLE FRICTION DAMPERS

B.R. Raut* and R.S. Jangid
Department of Civil Engineering, Indian Institute of Technology Bombay, Powai, Mumbai-400076, India

Received: 23 April 2014; **Accepted:** 10 October 2014

ABSTRACT

The seismic response of 20-story benchmark building with semi-active variable friction dampers (SAVFD) is investigated under various earthquake ground motions. A recently proposed predictive control algorithm is employed. A parametric study is carried out to arrive at optimum value of gain multiplier so as to have maximum response reduction. The numerical study is carried out for the benchmark building installed with SAVFD and compared with passive and uncontrolled case. The effectiveness of dampers is studied in terms of the reduction in structural responses and performance criteria. To reduce the cost of dampers study is carried out with lesser number of dampers at appropriate locations. Results show that SAVFD reduces earthquake responses effectively with better performance in respect of acceleration response reduction as compared with passive dampers. In addition, it is observed that the lesser number of dampers at appropriate locations results similar response reduction which reduces cost of the dampers.

Keywords: Benchmark building; earthquake excitation; seismic response; vibration control; semi-active variable friction damper; optimal locations.

1. INTRODUCTION

Vibrations induced by natural hazard of strong earthquakes have caused severe damage to mid to high-rise buildings located on the earthquake-threaten terrains. To protect these buildings from natural hazards and to make occupant feel safe and comfortable, structural control devices have been developed to dissipate the energy injected by earthquake forces thereby reducing vibrations in buildings. Structural control devices modify the dynamic properties of structures to undesirable excitations. A variety of structural control devices have been proposed and implemented which can be classified as passive, active and semi-

*E-mail address of the corresponding author: brraut@iitb.ac.in (B.R. Raut)

active devices [1, 2]. Passive control devices utilize the motion of structures to develop the control forces without requiring an external power source for their operations. Active control devices, on the other hand require a large power source to operate the actuators which supply the control forces. The magnitude of control forces are determined using feed-back from sensors that measure the excitation of structure. Semi-active control combines the features of active and passive systems. They utilize the response of a structure to develop control actions through the adjustment of damping or stiffness characteristics of the system.

Substantial progress has been made in the area of structural control in the past by using analytical and experimental studies on different buildings by various investigators for different dynamic loads. There was no common platform for comparison of results of reduction of responses of structures. Therefore, to compare, streamline and focus the study of structural control on the same building with the same dynamic loads, the concept of benchmark problem has come into picture. Benchmark control problems offer a set of carefully modeled real-world structures in which different control strategies can be implemented, evaluated, and compared using a common set of performance indices subject to same set of excitations. Such problems have been established to explore a successful development of structural control devices and algorithms. By using this concept of benchmark problem, the effectiveness of control devices and control algorithms can be easily compared. Therefore, based on realistic full-scale buildings, two structural control benchmark problems have been proposed for earthquake and wind excitations [3]. One such seismically excited benchmark problem is 20-story steel building designed by Brandow and Johnston Associates for Los Angeles, California region.

Performance of various control devices like active dampers in the form of hydraulic actuators [3], hybrid control scheme in the form of passive like viscous and yielding energy dissipation elements, active like tendon control and tune mass and semi-active like magnetorheological (MR) dampers [4], MR dampers [5] and filtered linear quadratic (LQ) optimal and $H_{infinity}$ based optimal control theory with suitable placement of actuators and sensors [6] on linear model of 20-story benchmark building have been studied. Yoshida and Dyke [7] applied semi-active control systems using MR dampers to a nonlinear model of a 20-story benchmark building to verify its effectiveness in reducing responses. Fukukita et al. [8] studied control effect for 20-story nonlinear benchmark building using passive viscous damping walls and semi-active variable oil dampers with linear quadratic Gaussian (LQG) control theory and demonstrated that both passive device and semi-active device can effectively reduce the response of the structure in various earthquake motions. Chen and Chen [9] studied responses of seismically excited nonlinear 20-story benchmark building with piezoelectric friction dampers by considering both stick and sliding phases of dampers. Kim et al. [10] investigated the behavior of nonlinear 20-story benchmark building employing MR dampers operated by a model-based fuzzy logic controller (MBFLC) formulated in terms of linear matrix inequalities (LMI).

A friction damper consists of the frictional sliding interface and a clamping mechanism that produces a normal contact force on the interface. The dry, sliding, solid friction that developed between two interfaces introduces static and dynamic coefficients which oppose the motion of the damper. The basic theory of friction damper is founded upon the Coulomb's friction law and has equal static and dynamic friction coefficients. Moreover the static and dynamic friction coefficients depends upon many factors such as physical and

chemical processes, bimetallic interface conditions, environmental factors etc. as such there is a need for much more reliance on physical testing. Aiken and Kelly [11] based on the matrix of component tests performed indicate that the response of friction dampers is extremely regular and repeatable with rectangular hysteresis loops. Furthermore, the effect of loading frequency and amplitude, number of cycles, or ambient temperature on damper response was reported to be negligible. Friction dampers are usually classified as one of the displacement-dependent energy dissipation devices and the damper force is independent of the velocity and frequency content of excitation [12]. Since the threshold slip force of the passive friction damper is pre-determined fixed value, it starts to slip and dissipate energy when the seismically exerted damper force exceeds the slip force. Otherwise an inactivated damper will be in stick state behaving as regular bracing system and there is no energy dissipation. Thus passive friction dampers, during an earthquake may switch between slip and stick states, which results in high frequency structural responses.

Semi-active dampers are proposed in the literature, to improve the performance of passive friction dampers. Semi-active friction damper is able to adjust its slip force by controlling its clamping force in real time, depending on the structure's motion during an earthquake. This adaptive nature makes a semi-active friction damper more efficient. In order to determine adjustable clamping forces of semi-active friction dampers, it requires a feedback control algorithm and online measurement of structural response. The performance of semi-active friction damper depends on the control algorithm used. Akbay and Aktan [13] proposed the control algorithm that determines the clamping force at the next time step. Other proposed control laws include the bang-bang control [14], modulated homogenous control [15], linear quadratic regulator [16], modal control [17,18], friction force incremental control [19], predictive control [20] and linear control [21]. Kori and Jangid [22] studied the performance of semi-active variable friction damper by placing them at various floors of multistoried building using predictive control law. Patil and Jangid [23] compared the effectiveness of semi-active variable friction dampers with passive linear viscous dampers with different damper placement configurations for wind excited benchmark building. It has been observed from above studies that the performance of SAVFD to control the seismic response of benchmark building not been investigated so far.

In this paper, the effectiveness of SAVFD in mitigating the seismic responses of benchmark building in terms of namely, displacement, acceleration, shear forces and the performance criteria stipulated in benchmark control problem under various earthquakes is investigated. The specific objective of the study are (i) to identify the optimum gain multiplier of SAVFD installed with benchmark building, (ii) to study hysteretic energy dissipation behavior, (iii) to compare the efficiency in terms of response quantities of the benchmark building installed with SAVFD with passive friction dampers, and (iv) to investigate optimum number/locations of dampers for minimizing cost of dampers.

2. BENCHMARK BUILDING

The 20-story structure used for seismically excited second generation benchmark control problem [3] as shown in Fig. 1 is designed for Los Angeles, California region. The building consists of basements at two levels and 20 upper floors having size 30.48 m x 36.58 m in

plan and 80.77 m in elevation above ground level. The building has five bays in north-south (N-S) direction and six bays in east-west (E-W) direction with bay width 6.10 m each. The lateral load of the building is resisted by steel perimeter moment resisting frames (MRFs) in both directions. The floor-to-floor height is 3.96 m for 19 upper floors, 5.49 m for first floor and 3.65 m for each basement. Adequately designed column splices are used after every three floors after second story. The column bases are modeled as pinned and horizontal displacement at first floor is assumed to be restrained. The building contains simple framing with composite floor of steel sections embedded in concrete slab. This composite floor provides diaphragm action assumed to be rigid in horizontal plane. The loads on account of steel framing, floor slabs, ceiling/flooring, mechanical/electrical, partitions, roofing and a penthouse located on the roof are specified in benchmark control problem. Each perimeter MRF resists one half of the seismic mass associated with entire structure. The shorter and weaker direction N-S MRF is considered for analysis. Because the focus of study is on global response characteristics, considering the linearized response of the structure can be shown to be a reasonable approximation [24]. Thus, the N-S MRF is modeled as two dimensional plane structures with linear elastic behavior in finite element method (FEM). The FEM model consists of 180 nodes and 284 elements with three degrees-of-freedoms (DOFs) per node thereby the entire structure is having 540 DOFs. The DOFs on account of boundary conditions are reduced to 526 DOFs. With the help of Ritz transformation, 526 DOFs are reduced to 418 DOFs by condensing out the DOFs on account of rigid diaphragm action of all floors.

The response contributions of all the natural modes must be considered if the exact structural response to dynamic excitation is desired, but the first few modes can usually provide sufficiently accurate results. More modes need to be included for response of shear force than for floor displacement because the modal contribution factors for higher modes are larger for shear force than for roof displacement. The natural frequencies of the higher modes in this model are excessively large. As these modes, attributed mostly to rotational and vertical DOFs, are unlikely to contribute to the response of the physical system, they are reduced out in order to reduce the model to manageable size so as to carry out dynamic analysis computationally unburdensome. Thus, the model is reduced to 106 DOFs by using Guyan reduction. From the typical transfer functions plots, it has been established that the results are consistent comparing reduced and full models. Thus, finally the nominal evaluation model is having 106 DOFs. The energy absorption and dissipation characteristics of the as build structure in reducing dynamic effects is known as inherent (natural) modal damping. The damping values are employed as per the prevailing codes [25]. In Japan, 1st mode damping ratios are used 2.0% in high rise steel buildings and 3.0% in reinforced concrete buildings in the design stage such as earthquake or wind action subject to maximum of 10%. And relations in the damping ratios of higher modes are proportional to associated natural frequencies. However, these values or relations have no theoretical reasons. Thus, the damping matrix is arrived by assuming damping in each mode proportional to mode's frequency subject to maximum of 10% of critical damping in any one mode with 2% damping in first mode. The first 10 natural frequencies of this nominal model are: 0.26, 0.75, 1.30, 1.83, 2.40, 2.80, 3.00, 3.21, 3.63 and 4.31 Hz.

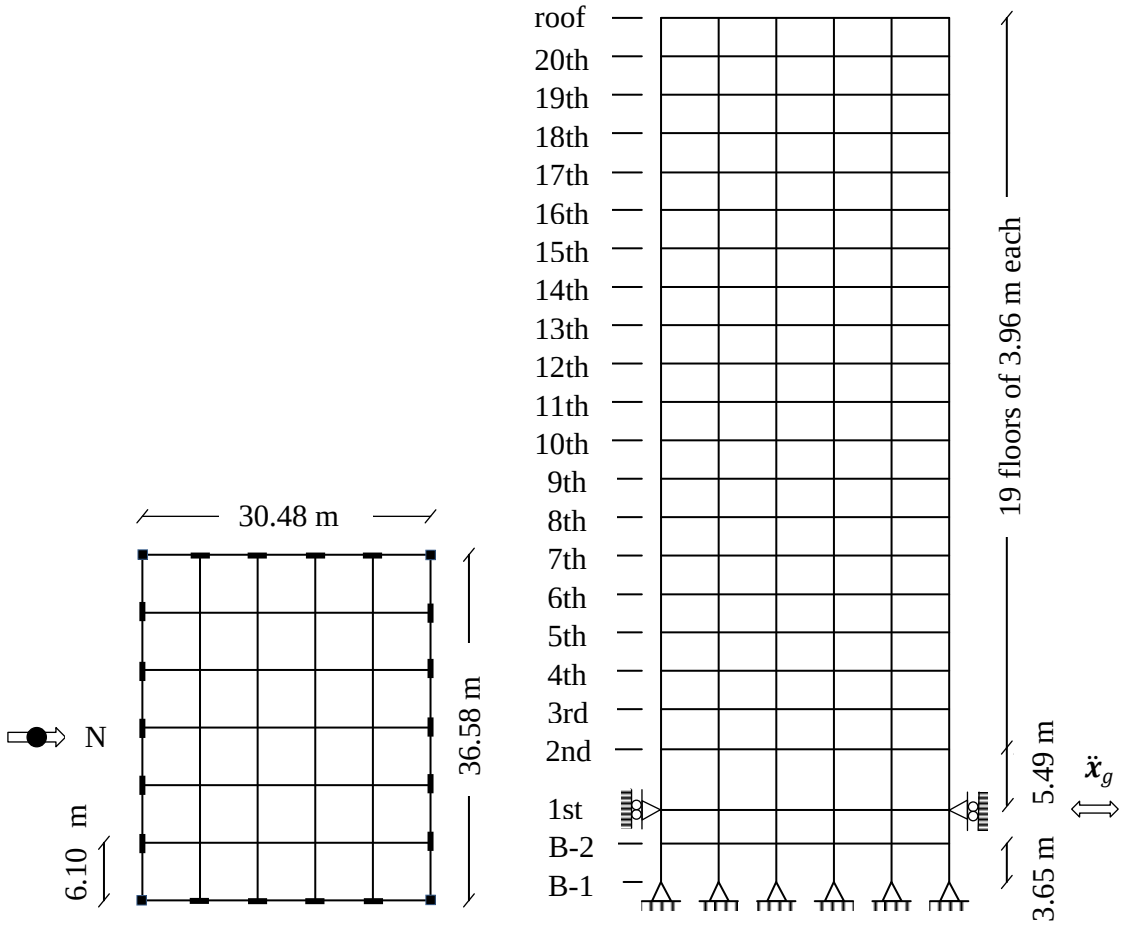

(a) Plan (b) Elevation

Figure 1. The seismically excited benchmark building [3]

In this benchmark problem, two evaluation models have been proposed [3] based on change of dynamic properties of building from before to after strong motion earthquake [24]. These two evaluation models are pre-earthquake evaluation model and post-earthquake evaluation model respectively. The presence of non-structural elements of building such as partition walls and cladding add some stiffness to the structure, since finite element model has been derived without considering stiffness effect of non-structural elements. The cognizance of this additional stiffness is taken in pre-earthquake evaluation model by increasing the stiffness of nominal model proportionally such that first natural frequency of the model is 10% greater than that of nominal model. The damping is derived accordingly based on increased stiffness. After a strong motion earthquake, the non-structural elements may no longer provide any additional stiffness to the structure. Moreover, the structural elements may be damaged, causing a decrease in stiffness. Thus, the post-earthquake evaluation model is arrived at by decreasing the stiffness of nominal model on account of this stiffness degradation, such that natural frequency of the structure is decreased by 10% of nominal model. The damping is derived from decreased stiffness accordingly. It is to be

stated that the post-earthquake evaluation model assumes structural damage has occurred, which may be potentially avoided through the application of control devices. Therefore, the post-earthquake building model may be viewed in some sense as representing a "worst-case" scenario. The first 10 natural frequencies of the pre-earthquake evaluation model are: 0.29, 0.83, 1.43, 2.01, 2.64, 3.08, 3.30, 3.53, 3.99 and 4.74 Hz. The first 10 natural frequencies of the post-earthquake evaluation model are: 0.24, 0.68, 1.17, 1.65, 2.16, 2.52, 2.70, 2.89, 3.26 and 3.88 Hz.

2.1 Performance criteria

To assess the merit of the control strategy, in this benchmark problem, fifteen performance criteria based on maximum response quantities, normed measure responses, number of sensors, control devices and the total power required by the control system are specified [3]. Smaller values of these performance criteria are generally more desirable. The first four performance criteria J_1 - J_4 deal with maximum responses such as relative displacement, inter-story drift, absolute acceleration and base shear respectively of the benchmark building. Additional four performance criteria J_5 - J_8 are stipulated based on L_2-normed measures. These are normed relative displacement, normed inter-story drift, normed absolute acceleration and normed base shear respectively. Performance criterion J_9 deals with maximum control force and J_{10} deals with maximum stroke of control devices. The performance criterion J_{11} and J_{12} deals with total power and normed power required by the control devices respectively. The performance criterion J_{13} , J_{14} and J_{15} deal with number of control devices, number of sensors and computational resources required to implement control algorithm respectively. Among these fifteen criteria, ten criteria J_1 - J_{10} are evaluated in this study. The summary of performance criteria J_1 - J_{10} with expressions defined for the benchmark building is given in Table 1.

Table 1: Performance criteria of the benchmark building

Floor Displacement	Normed Interstory Drift
$J_1 = \max_{\substack{\text{El Centro}\\ \text{Hachinohe}\\ \text{Northridge}\\ \text{Kobe}}} \left\{ \frac{\max_{\substack{t\\ i\epsilon\eta}} \lvert X_i(t) \rvert}{x^{max}} \right\}$	$J_6 = \max_{\substack{\text{El Centro}\\ \text{Hachinohe}\\ \text{Northridge}\\ \text{Kobe}}} \left\{ \frac{\max_{t,i} \frac{\lVert d_i(t) \rVert}{h_i}}{\lVert d_n^{max} \rVert} \right\}$
Interstory Drift	Normed floor Acceleration
$J_2 = \max_{\substack{\text{El Centro}\\ \text{Hachinohe}\\ \text{Northridge}\\ \text{Kobe}}} \left\{ \frac{\max_{t,i} \frac{\lvert d_i(t) \rvert}{h_i}}{d_n{}^{max}} \right\}$	$J_7 = \max_{\substack{\text{El Centro}\\ \text{Hachinohe}\\ \text{Northridge}\\ \text{Kobe}}} \left\{ \frac{\max_{i\epsilon\eta} \lVert \ddot{x}_{ai}(t) \rVert}{\lVert \ddot{X}_a^{max} \rVert} \right\}$
Floor Acceleration	Normed Base Shear
$J_3 = \max_{\substack{\text{El Centro}\\ \text{Hachinohe}\\ \text{Northridge}\\ \text{Kobe}}} \left\{ \frac{\max_{\substack{t\\ i\epsilon\eta}} \lvert \ddot{X}_{ai}(t) \rvert}{\ddot{X}_a{}^{max}} \right\}$	$J_8 = \max_{\substack{\text{El Centro}\\ \text{Hachinohe}\\ \text{Northridge}\\ \text{Kobe}}} \left\{ \frac{\left\lVert \sum_{i=1}^{20} m_i \ddot{x}_{a\eta i}(t) \right\rVert}{\lVert F_b^{max} \rVert} \right\}$
Base Shear	Control Force

$J_4 = \max_{\substack{\text{El Centro}\\ \text{Hachinohe}\\ \text{Northridge}\\ \text{Kobe}}} \left\{ \frac{\max_{t} \lvert \sum_{i=1}^{20} m_i \ddot{x}_{a\eta i}(t) \rvert}{F_b{}^{max}} \right\}$	$J_9 = \max_{\substack{\text{El Centro}\\ \text{Hachinohe}\\ \text{Northridge}\\ \text{Kobe}}} \left\{ \frac{\max_{t,i} \lvert f^i(t) \rvert}{W} \right\}$
Normed floor Displacement	Control Device Stroke
$J_5 = \max_{\substack{\text{El Centro}\\ \text{Hachinohe}\\ \text{Northridge}\\ \text{Kobe}}} \left\{ \frac{\max_{i\epsilon\eta} \lVert X_i(t) \rVert}{\lVert X^{max} \rVert} \right\}$	$J_{10} = \max_{\substack{\text{El Centro}\\ \text{Hachinohe}\\ \text{Northridge}\\ \text{Kobe}}} \left\{ \frac{\max_{t,i} \lvert y_i^a(t) \rvert}{x^{max}} \right\}$

2.2 Seismic ground motions

In this benchmark problem, in order to examine the behavior of the benchmark building, four different earthquake time histories are stipulated. Those are: El Centro, 1940; Hachinohe, 1968; Northridge, 1994 and Kobe, 1995. These four ground motions are suggested by the International Association on Structural Control for benchmark control problems. The data for these four ground motions such as time history, peak ground acceleration (PGA), recording station and distance from epicenter are available. These earthquake time histories are classed as strong, modest and severe based on intensity of the earthquake. The El Centro, 18 May 1940, N00S component, earthquake is recorded at Imperial Valley irrigation district substation California, took place at a distance of 11.58 km from the epicenter having 0.348g (g acceleration due to gravity) PGA lasted for 50 sec belongs to strong earthquake class. The Hachinohe, 16 May 1968, N90E component, earthquake is recorded at Hachinohe city, during the Takochi-oki, took place at a distance of 26 km from the epicenter having 0.25g PGA lasted for 36 sec belongs to modest class. The Northridge, 17 January 1994, N00E component, earthquake is recorded at Sylmar County Hospital parking lot, took place at a distance of 19 km from the epicenter having 0.843g PGA lasted for 60 sec belong to severe class. The Kobe, 17 January 1995, N90E component, earthquake is recorded at JMA (Japan Meteorological Agency) station, took place at a distance of 17 km from the epicenter having 0.834g PGA lasted for 150 sec belongs to severe class.

2.3 Governing equations of motion

The governing equations of motion for 106 DOFs controlled benchmark building evaluation model subject to seismic excitations can be written as

$$M\ddot{x} + C\dot{x} + Kx = -M\Gamma\ddot{x}_g + Pu \tag{1}$$

where M, C and K are mass, damping and stiffness matrices respectively of finite element evaluation model of benchmark building each is having size of 106×106. x is the floor displacement relative to ground vector, $\dot{x}$ and $\ddot{x}$ are the floor velocity and acceleration vectors, respectively. $u = [f_{d1,}\ f_{d2,}\ f_{d3}\ \ldots\ldots f_{dr}]^T$ is the vector of damper forces input and $\ddot{x}_g$ (m/sec^2) is the ground acceleration. Γ is a vector of zeros and ones defining loading of the ground acceleration to the structure, P is a vector defining how the forces produced by the control device enter the structure. Responses for a particular level are measured at the

floor of the level in question.

The equations of motion (Equation 1) can be rewritten in the state-space form as

$$\dot{z} = Az + Bu + E\ddot{x}_g \tag{2}$$

where

$$A = \begin{bmatrix} 0 & I \\ -M^{-1}K & -M^{-1}C \end{bmatrix}; \quad B = \begin{bmatrix} 0 \\ M^{-1}P \end{bmatrix}; \quad E = \begin{bmatrix} 0 \\ -\Gamma \end{bmatrix} \tag{3}$$

where z is the state vector of structure and contains displacement and velocity of each DOF; A denotes the system matrix composed of structural mass, damping and stiffness matrices; B represents the distributing matrix of the control forces; and E represents the distributing matrix of seismic load excitation.

The state space equation (Equation 2) is discretized in the time domain and excitation force is assumed to be constant at any time within the interval and can be written into a discrete-time form [26]

$$z[k+1] = A_d z[k] + B_d u[k] + E_d \ddot{x}_g[k] \tag{4}$$

where a variable (z, u, $\ddot{x}_g$) followed by $[k]$ or $[k+1]$ denotes that the variable is evaluated at the k-th or the $(k+1)$-th time step. $A_d = e^{A\Delta t}$ represents the discrete time system matrix with Δt as the time interval and

$$B_d = A^{-1}(A_d - I)B \tag{5}$$
$$E_d = A^{-1}(A_d - I)E \tag{6}$$

2.4 Semi-active variable friction dampers

Variable friction damper is one of the promising semi-active devices for seismic protection. In order to improve the performance of friction damper device (FDD), the concept of semi-active control is introduced [13, 20] to the passive friction dampers. The schematic and mathematical model of semi-active variable friction damper is shown in Fig. 2. A semi-active friction damper is able to adjust its slip force by controlling its clamping force

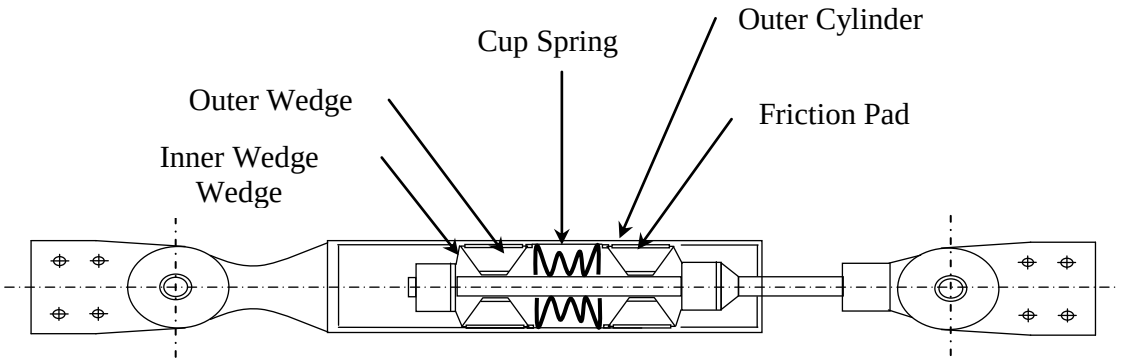

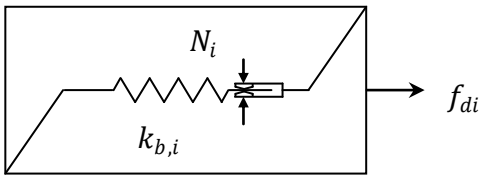

Figure 2. Schematic and mathematical model of semi-active variable friction damper [22]

In real time in response to a structure's motion during earthquake. The required clamping force is provided through the action of the spring against the inner and outer wedges with the help of piezoelectric actuators as detailed in [27]. The working operations and dynamics of actuator are not covered in the present study. Because of this adaptive nature of active control, a semi-active friction damper is expected to be more effective than a passive damper. The control of semi-active friction dampers requires a feedback control algorithm and online measurements of structural response which are required to determine the appropriate level of adjustable clamping forces of the dampers. Semi-active variable friction damper requires less power, since control action is carried out by adjusting clamping force. In addition, because it does not pump energy into the controlled structures, control instability can be prevented by semi-active variable friction dampers. However, the control performance of the semi-active dampers significantly relies on the control algorithm applied. One of the recent control laws, 'predictive control law' [20] is used here. This control law determines the frictional force for the next time step required to keep the dampers continuously slipping and is given by

$$u[k] = \alpha \left(G_z z[k-1] + G_u u[k-1] + G_w \ddot{x}_g[k-1]\right) \tag{7}$$

where α is a gain multiplier defined as the ratio of damper force to critical damper control force and plays an important role in the present control law.

$$G_z = K_b D(A_d - I) \tag{7a}$$
$$G_u = K_b D B_d + I \tag{7b}$$
$$G_w = K_b D E_d \tag{7c}$$

After being multiplied by the factor α, these matrices G_z, G_u, G_w may also be treated as the control gains. K_b is (r x r) diagonal matrix where i^{th} diagonal element $k_{b,i}$ is the stiffness of i^{th} damper and r number of dampers used in this control strategy.

Let y be a vector listing all damper elongations (deformations) that are equal to the drifts of the stories on which the dampers are installed. At any given instant in time, the relation between y and the state of the structure z may be written as

$$y[k] = Dz[k] \tag{7d}$$

where D is the constant matrix.

3. NUMERICAL STUDY

In the numerical study, two evaluation models viz. pre-earthquake evaluation model and post-earthquake evaluation model of benchmark building are considered. The earthquake ground motions used to evaluate the seismic behavior of the benchmark building models are: El Centro; Hachinohe; Northridge and Kobe earthquakes. The details of the ground motions are explained. Though the duration of above ground motions is ranging from 36 sec to 150 sec, in this study numerical simulation is required to be carried out for sufficiently large time to allow the response of the model to attenuate to less than 0.1% of its maximum value. As such to arrive at normed responses, the simulation is carried out for 100 sec for El Centro, Hachinohe and Northridge earthquakes and 180 sec for Kobe earthquake. In order to check the feasibility of the control system, numerical simulations are carried out first for uncontrolled models with inherent viscous damping. The maximum uncontrolled response of inter-story drift is found for post-earthquake evaluation model subject to Northridge earthquake as 1.85% that is much larger than 0.5%. The maximum uncontrolled floor acceleration is found for pre-earthquake evaluation model subject to Northridge earthquake as 9.19 m/sec^2 that is also much larger than 0.7g. These aspects justify the need of implementing control system.

The performance of SAVFD using predictive control law with complete state feedback with the dampers installed on all floors of benchmark building is investigated and compared with the uncontrolled and passive friction case. The stiffness of each SAVFD bracing is considered as 1.728e^5 kN/m. A thorough study is conducted to arrive at optimum damper parameters in the SAVFD for benchmark building with both the models subject to four different earthquake ground motions. Since the efficiency of SAVFD by using predictive control algorithm depends on selection of gain multiplier which is ratio of clamping force to critical damping force, the gain multiplier is investigated. To arrive at the optimum gain multiplier of the SAVFD installed on all floor levels of the benchmark building, the variation of the top floor relative displacements, top floor absolute accelerations, and base shears of the two models for all four earthquakes are plotted as shown in the Fig. 3. It shows the influence of the gain multiplier on the peak responses under different earthquake ground motions. It is observed that the responses of both the models are reduced up to a certain value of the gain multiplier and, later on, they increase again. Thus, it implies that the optimum gain multiplier value exists to yield the lowest responses of both the models. As the optimum gain multiplier is not the same for both the models, the optimum value is taken as one, which gives the lowest displacement and base shear responses of both the models, with no increase in accelerations. It is observed that the optimum value of the gain multiplier is 0.99 considering both the models for all four earthquakes.

A thorough study is also conducted to arrive at the optimum slip force of the friction dampers installed with benchmark building models under the various earthquake excitations described earlier. The slip force was normalized with the weight of the structure to get the normalized slip force. To arrive at the optimum slip force in the friction dampers, the variations of the responses of both the models are plotted with the normalized slip force for all four earthquakes considered. This plotting is shown in Fig. 4. The normalized slip force for the optimum responses is found to be 0.007.

The time history of the top floor displacement responses of the two models without

dampers, with the passive friction damper of optimum slip force and with the SAVFD of the optimum gain multiplier obtained above, are shown in Fig. 5. The effectiveness of the passive friction damper and SAVFD in reducing the acceleration and base shear can be noticed from Fig. 6 and Fig. 7, which show the time history of the acceleration and base shear of two models without dampers, installed with friction dampers of optimum slip force and installed with SAVFD of the optimum gain multiplier. These time histories plots are shown for 80 sec for El Centro, Hachinohe and Northridge ground motions and 100 sec for Kobe ground motion. These figures clearly indicate the effectiveness of SAVFD in mitigating the earthquake responses of both the models.

A larger value of the gain multiplier will lead to higher control force, and therefore results in better energy dissipation of the benchmark building. The damper force and damper displacement of the SAVFD of the optimum gain multiplier under different earthquakes, for pre-earthquake evaluation model for the 20th floor damper, is shown in Fig. 8. It is observed that during all earthquake ground motions, SAVFD is more effective for energy dissipation.

Figs. 9 and 10 show the variation of the displacement and shear forces, respectively, along height of models for three different cases: uncontrolled, installed with passive friction dampers of the optimum slip force, and installed with SAVFD of the optimum gain multiplier. It shows the ability of SAVFD and passive friction dampers to mitigate the displacement and shear-force of benchmark building. The reductions in the peak top floor displacements, peak top floor absolute accelerations, and the normalized base shears of the two models without dampers, installed with passive dampers of optimum slip force and with SAVFD of optimum gain multiplier, are reported in Table 2. From the Table 2, it is observed that the performance of benchmark building installed with SAVFD against acceleration is better than that of against displacement as compared to passive friction dampers.

For pre-earthquake evaluation model, SAVFD reduces top floor absolute acceleration by 65.22% as against 27.14% with passive friction dampers for El Centro earthquake. Similarly reduction of top floor acceleration in case of Hachinohe earthquake is 41.64% as against 10.66%, for Northridge earthquake 52.77% as against 2.65% and for Kobe earthquake 71.77% as against 8.95%. Similar trend is observed for post-earthquake evaluation model. SAVFD reduces top floor absolute acceleration by 71.73% as against 24.32% with passive friction dampers for El Centro earthquake. For Hachinohe earthquake, the reduction in top floor absolute acceleration is 49.42% as against 23.55% and for Northridge earthquake it is 64.39% as against 6.28%. For Kobe earthquake SAVFD reduces top floor absolute acceleration by 81.94% as against 21.92% with passive friction dampers. From these values it is found that SAVFD control strategy is very much effective in acceleration reduction as compared to passive friction damper as against displacement reduction. The hysteresis loops of SAVFD for single DOF system subject to harmonic load [20] appear to be very close to linear viscous damper. As such effectiveness of benchmark building installed with SAVFD is compared with passive viscous damper. For passive viscous damper installed control strategy [8] the maximum absolute acceleration among all four earthquakes is reduced by 20.24% with nonlinear model of benchmark building, whereas SAVFD control strategy with linear model is able to reduce maximum absolute acceleration to 21.50%. Therefore more advanced damping methods in the form of SAVFD is justifiable.

In order to minimize the cost of dampers, the responses of the benchmark building

models are investigated by considering 15 number of SAVFDs installed on 1, 2, 3, 4, 10, 11, 12, 13, 14, 15, 16, 17, 18, 19 and 20th floors. The dampers are placed on the floors with the maximum relative displacement and/or velocity. Figs. 11 and 12 show the variation of the displacement and shear forces, respectively, along the height of both the models for four different cases: case (i) uncontrolled, case (ii) installed with passive friction dampers of optimum slip force on all floors, case (iii) installed with SAVFDs on all floors, and case (iv) installed with SAVFDs on above 15 floors. When the SAVFDs installed on 15 floors, the displacement and shear forces in all stories were reduced almost as much as when they were installed on all floors. The reductions in the peak top floor displacement, peak top floor absolute accelerations, and the normalized base shear of the two models without dampers, installed with passive friction dampers and SAVFDs on 15 floors, are shown in Table 3. From the Table 3, it is observed that the performance of benchmark building installed with SAVFD against acceleration is better than that of against displacement as compared with passive friction dampers. For pre-earthquake evaluation model, SAVFD reduces top floor absolute acceleration by 62.23% as against 24.94% with passive friction dampers for El Centro earthquake. Similarly reduction of acceleration in case of Hachinohe earthquake is 39.84% as against 11.69%, for Northridge earthquake 49.84% as against 2.59% and for Kobe earthquake 70.25% as against 4.98%. Similar trend is observed for post-earthquake evaluation model. SAVFD reduces top floor absolute acceleration by 69.47% as against 37.04% with passive friction dampers for El Centro earthquake. For Hachinohe earthquake, the reduction in top floor absolute acceleration is 47.40% as against 22.89% and for Northridge earthquake it is 61.84% as against 8.97%. For Kobe earthquake SAVFD reduces top floor absolute acceleration by 80.72% as against 12.90%. From these values it is found that SAVFD control strategy with less number of dampers at appropriate locations is also very much effective in acceleration reduction as compared to passive friction damper counterpart as against displacement reduction. From Tables 2 and 3, it is observed that the response reduction of the two models with 15 number of FDDs and SAVFDs is almost as much as of that obtained for the models with dampers installed with all the floors. Thus, it can be concluded that instead of providing dampers at all floors, even providing less number of dampers may result in the same structural performances during earthquakes, which reduces cost of dampers.

To compare the effectiveness of SAVFD installed control strategy with that of sample controller [3], performance criteria are investigated and reported in Table 4 and 5 for both pre-earthquake and post-earthquake evaluation model respectively. The values of performance criteria J_1 - J_{10} for sample controller with active control in the form of 50 hydraulic actuators for pre-earthquake evaluation model are: 0.8417, 0.8906, 0.9087, 0.9295, 0.6983, 0.7319, 0.6215, 0.7015, 0.0014, and 0.1001 and for post-earthquake evaluation model are: 0.957, 0.952, 0.989, 1.024, 0.642, 0.626, 0.723, 0.587, 0.013, and 0.098. The results obtained in this study of SAVFD controlled system with 20 dampers as arrived in Table 4 and 5 (column 10) are quite comparable with the sample controller with both the

Table 2: Peak response quantities of the benchmark building installed with SAVFD on all floors

Earthquake	Evaluation Model	Response quantities								
		Top floor displacement (cm)			Top floor acceleration (g)			Normalized base shear		
		Uncont-rolled	FDD on all floors	SAVFD on all floors	Uncont-rolled	FDD on all floors	SAVFD on all floors	Uncont-rolled	FDD on all floors	SAVFD on all floors
El Centro, 1940	Pre-earthquake	37.943	29.061 (23.41)#	29.593 (22.00)	0.318	0.231 (27.14)	0.111 (65.22)	0.080	0.067 (15.22)	0.070 (12.58)
	Post-earthquake	27.779	22.641 (18.50)	23.743 (14.53)	0.226	0.171 (24.32)	0.064 (71.73)	0.038	0.042 (-8.62)	0.043 (-11.23)
Hachinohe, 1968	Pre-earthquake	51.705	27.555 (46.71)	38.355 (25.82)	0.290	0.259 (10.66)	0.169 (41.64)	0.099	0.066 (33.54)	0.066 (32.93)
	Post-earthquake	29.828	25.349 (15.02)	29.609 (0.74)	0.198	0.152 (23.55)	0.100 (49.42)	0.049	0.052 (-6.76)	0.046 (6.76)
Northridge, 1994	Pre-earthquake	105.826	93.295 (11.84)	86.196 (18.55)	0.934	0.909 (2.65)	0.441 (52.77)	0.204	0.189 (7.02)	0.187 (8.15)
	Post-earthquake	90.685	87.083 (3.97)	72.712 (19.82)	0.792	0.742 (6.28)	0.282 (64.39)	0.147	0.154 (-4.76)	0.163 (-10.94)
Kobe, 1995	Pre-earthquake	56.862	49.043 (13.75)	41.777 (26.53)	0.910	0.828 (8.95)	0.257 (71.77)	0.174	0.129 (25.48)	0.109 (36.95)
	Post-earthquake	65.610	48.047 (26.77)	47.323 (27.87)	0.738	0.576 (21.92)	0.133 (81.94)	0.115	0.108 (5.33)	0.120 (-4.89)

quantity within the parentheses denotes percentage reduction

Table 3: Peak response quantities of the benchmark building installed with SAVFD on 15 floors

Earthquake	Evaluation Model	Response quantities								
		Top floor displacement (cm)			Top floor acceleration (g)			Normalized base shear		
		Uncont-rolled	FDD on 15 floors	SAVFD on 15 floors	Uncont-rolled	FDD on 15 floors	SAVFD on 15 floors	Uncont-rolled	FDD on 15 floors	SAVFD on 15 floors
El Centro, 1940	Pre-earthquake	37.943	31.701 (16.45)#	31.450 (17.11)	0.318	0.238 (24.94)	0.120 (62.23)	0.080	0.063 (20.50)	0.070 (12.45)
	Post-earthquake	27.779	24.606 (11.43)	24.878 (10.44)	0.226	0.142 (37.04)	0.069 (69.47)	0.038	0.045 (-17.75)	0.040 (-3.39)
Hachinohe, 1968	Pre-earthquake	51.705	33.503 (35.20)	41.434 (19.86)	0.290	0.256 (11.69)	0.174 (39.84)	0.099	0.075 (24.34)	0.072 (26.97)
	Post-earthquake	29.828	28.374 (4.88)	29.466 (1.21)	0.198	0.153 (22.89)	0.104 (47.40)	0.049	0.055 (-12.09)	0.045 (6.97)
Northridge, 1994	Pre-earthquake	105.826	94.561 (10.64)	90.044 (14.91)	0.934	0.909 (2.59)	0.468 (49.84)	0.204	0.183 (10.31)	0.187 (8.20)
	Post-earthquake	90.685	87.637 (3.36)	76.481 (15.66)	0.792	0.721 (8.97)	0.302 (61.84)	0.147	0.146 (0.75)	0.157 (-6.79)
Kobe, 1995	Pre-earthquake	56.862	49.582 (12.80)	42.502 (25.25)	0.910	0.864 (4.98)	0.271 (70.25)	0.174	0.134 (22.77)	0.103 (40.92)
	Post-earthquake	65.610	49.969 (23.84)	51.931 (20.85)	0.738	0.643 (12.90)	0.142 (80.72)	0.115	0.112 (2.10)	0.118 (-2.62)

quantity within the parentheses denotes percentage reduction

Table 4: Performance criteria of the benchmark building installed with SAVFD (pre-earthquake evaluation model)

	El Centro		Hachinohe		Northridge		Kobe		Max Value	
	SAVFD on all floors	SAVFD on 15 floors	SAVFD on all floors	SAVFD on 15 floors	SAVFD on all floors	SAVFD on 15 floors	SAVFD on all floors	SAVFD on 15 floors	SAVFD on all floors	SAVFD on 15 floors
J_1	0.7799	0.8289	0.7418	0.8014	0.8145	0.8509	0.7347	0.7475	0.8145	0.8509
J_2	0.6936	0.7260	0.7374	0.7831	0.9513	0.9933	0.6586	0.6908	0.9513	0.9933
J_3	0.7850	0.8189	0.5911	0.6016	0.7184	0.7097	0.6460	0.6841	0.7850	0.8189
J_4	0.8742	0.8747	0.6700	0.7303	0.9187	0.9182	0.6304	0.5905	0.9187	0.9182
J_5	0.6749	0.7410	0.7104	0.7743	0.6409	0.7051	0.8656	0.8882	0.8656	0.8882
J_6	0.6435	0.7097	0.6876	0.7611	0.6404	0.7166	0.8463	0.8555	0.8463	0.8555
J_7	0.5193	0.5375	0.6456	0.7037	0.5603	0.6200	0.5329	0.5531	0.6456	0.7037
J_8	0.6043	0.6591	0.6541	0.7255	0.5847	0.6522	0.7685	0.7735	0.7685	0.7735
J_9	0.0624	0.0551	0.0280	0.0262	0.1476	0.1284	0.1632	0.1371	0.1632	0.1371
J_{10}	0.0526	0.0590	0.0568	0.0634	0.0739	0.0797	0.0849	0.0776	0.0849	0.0797

Table 5: Performance criteria of the benchmark building installed with SAVFD (post-earthquake evaluation model)

	El Centro		Hachinohe		Northridge		Kobe		Max Value	
	SAVFD on all floors	SAVFD on 15 floors	SAVFD on all floors	SAVFD on 15 floors	SAVFD on all floors	SAVFD on 15 floors	SAVFD on all floors	SAVFD on 15 floors	SAVFD on all floors	SAVFD on 15 floors
J_1	0.8547	0.8956	0.9926	0.9879	0.8018	0.8434	0.7213	0.7915	0.9926	0.9879
J_2	0.7087	0.7549	0.9366	0.9000	0.7809	0.8276	0.5640	0.6124	0.9366	0.9000
J_3	0.8843	0.9243	0.8148	0.8462	0.8093	0.8181	0.7415	0.7904	0.8843	0.9243
J_4	1.1120	1.0325	0.9341	0.9315	1.1097	1.0680	1.0490	1.0263	1.1120	1.0680
J_5	0.5923	0.6441	0.7382	0.7802	0.6150	0.6738	0.5661	0.6403	0.7382	0.7802
J_6	0.5996	0.6451	0.7182	0.7661	0.5592	0.6127	0.5734	0.6402	0.7182	0.7661
J_7	0.6902	0.7160	0.6580	0.7032	0.4842	0.4898	0.5493	0.5653	0.6902	0.7160
J_8	0.4310	0.4470	0.6795	0.7438	0.5159	0.5499	0.5599	0.6123	0.6795	0.7438
J_9	0.0589	0.0516	0.0253	0.0245	0.1357	0.1255	0.1583	0.1336	0.1583	0.1336
J_{10}	0.0654	0.0616	0.0942	0.0905	0.0869	0.0820	0.0671	0.0728	0.0942	0.0905

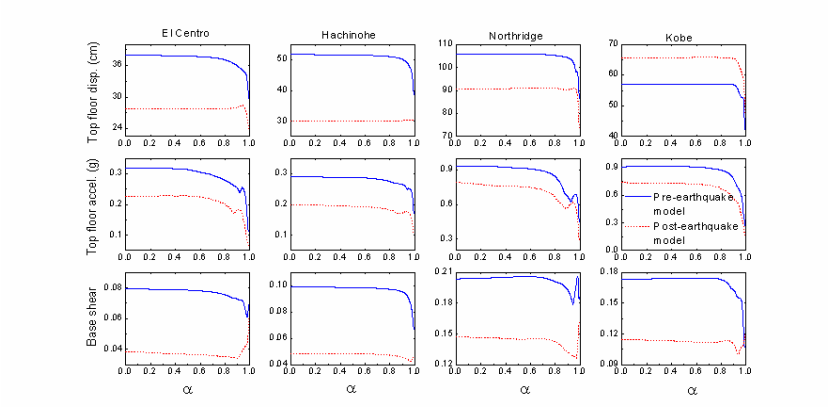

Figure 3. Variation of peak responses of two models against damper force gain multiplier when installed with SAVFD

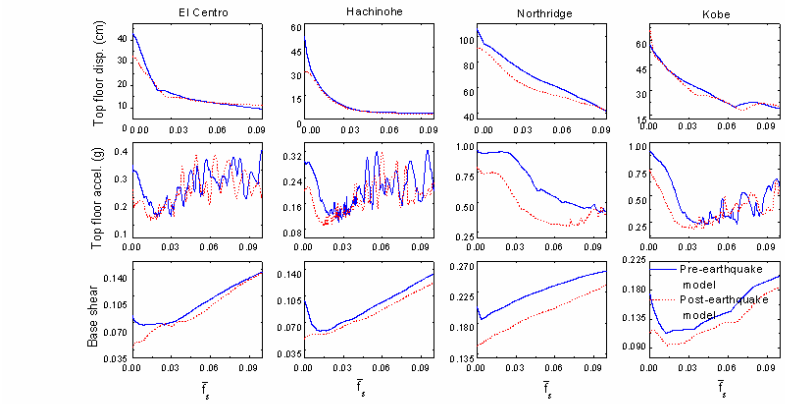

Figure 4. Variation of peak responses of two models against normalized slip force when installed with friction dampers

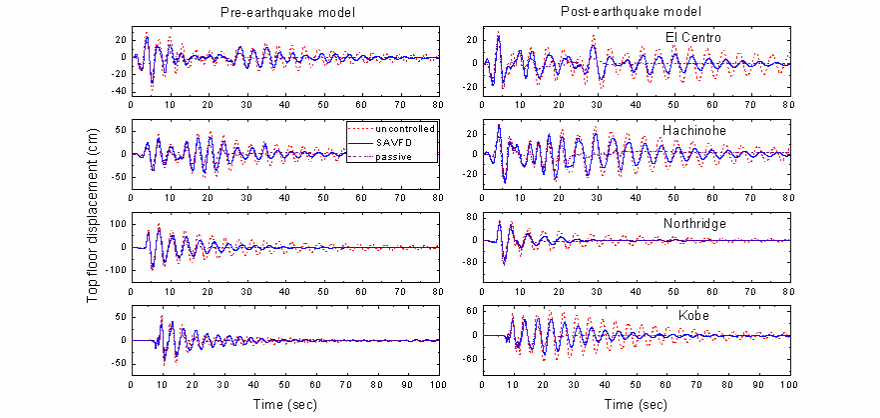

Figure 5. Time histories of top floor displacements of both the models

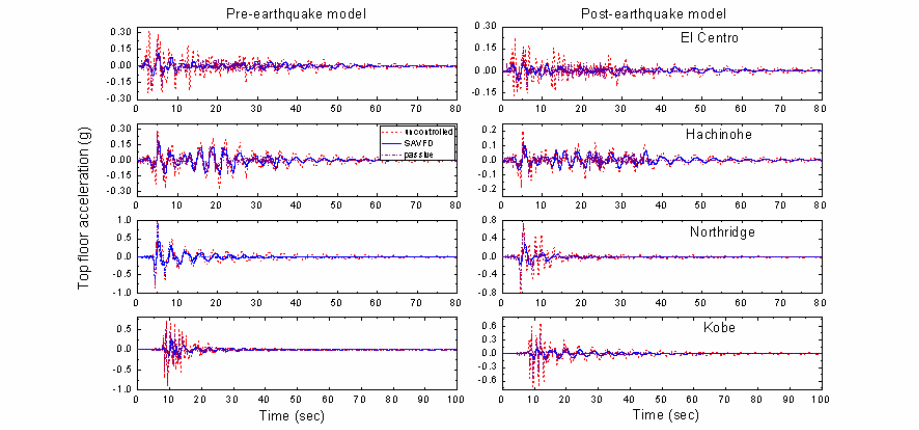

Figure 6. Time histories of top floor accelerations of both the models

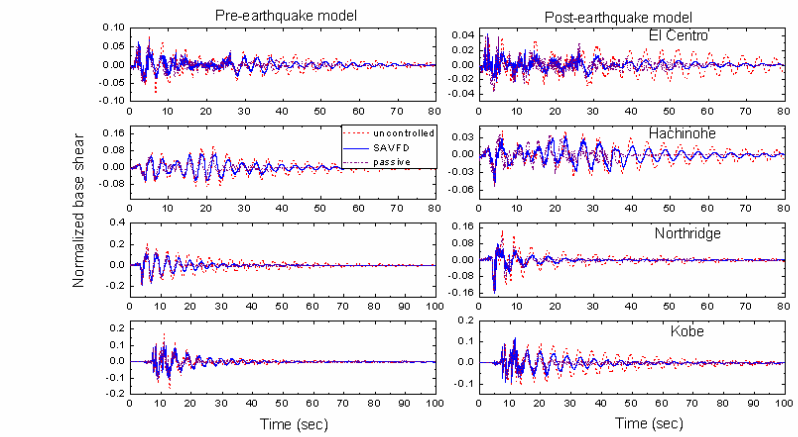

Figure 7. Time histories of normalized base shear of both the models

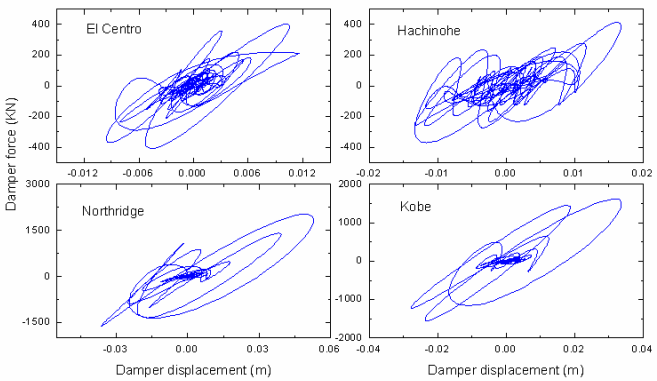

Figure 8. Control force displacement diagrams for 20th floor SAVFD under different earthquakes

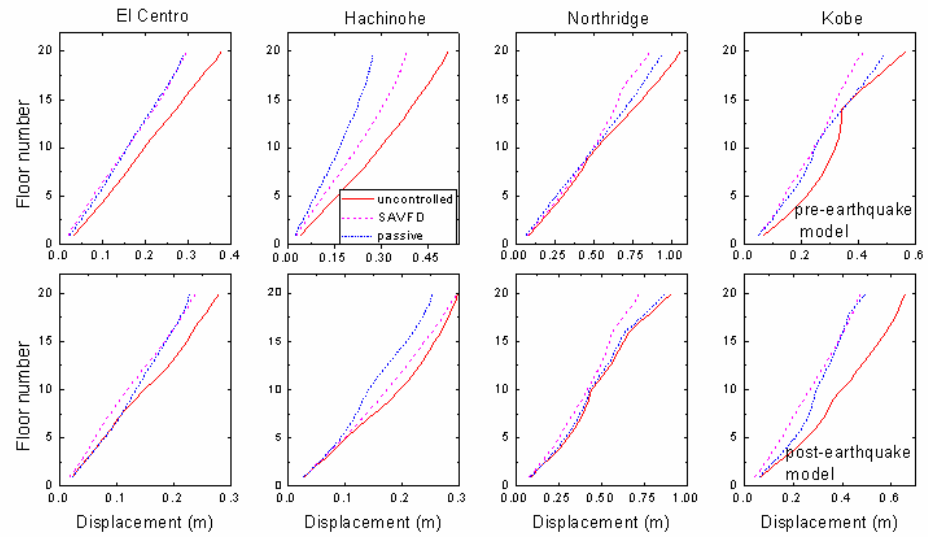

Figure 9. Variation of floor displacement along the height of both the models

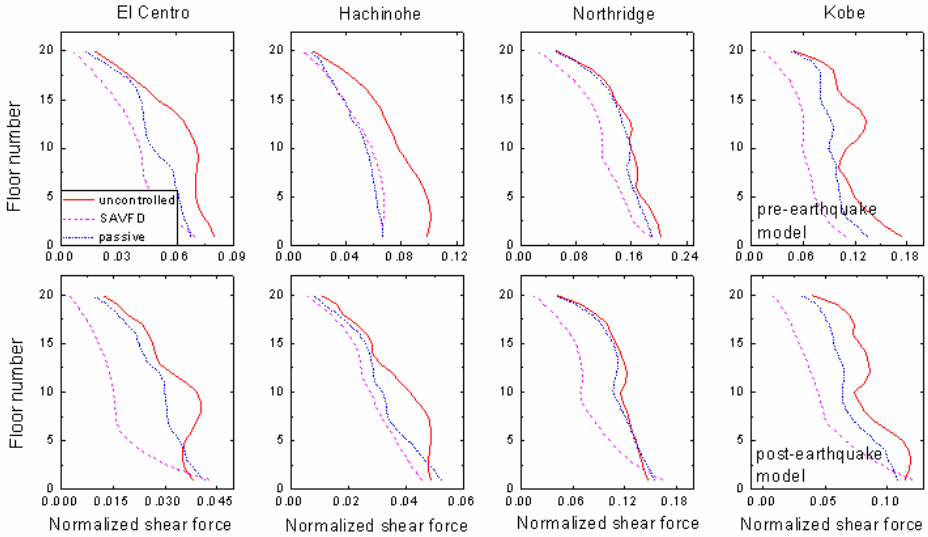

Figure 10. Variation of shear force along the height of both the models

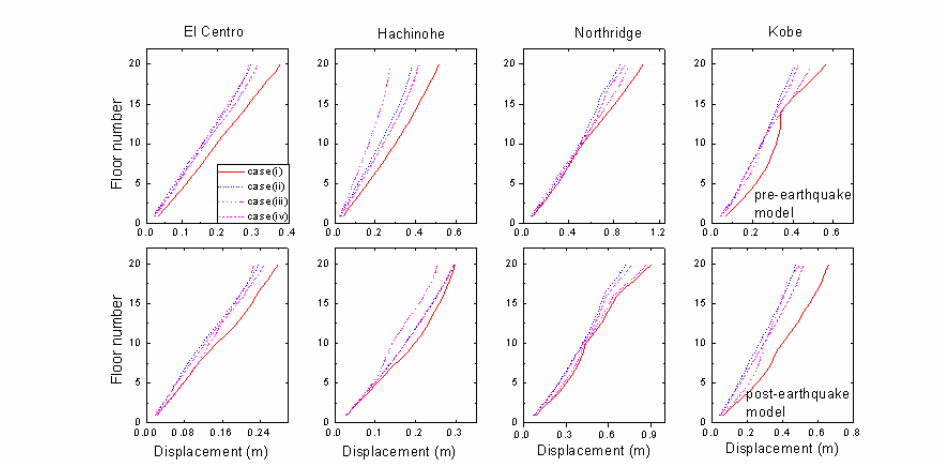

Figure 11. Comparison of floor displacements considering 15 no. of dampers

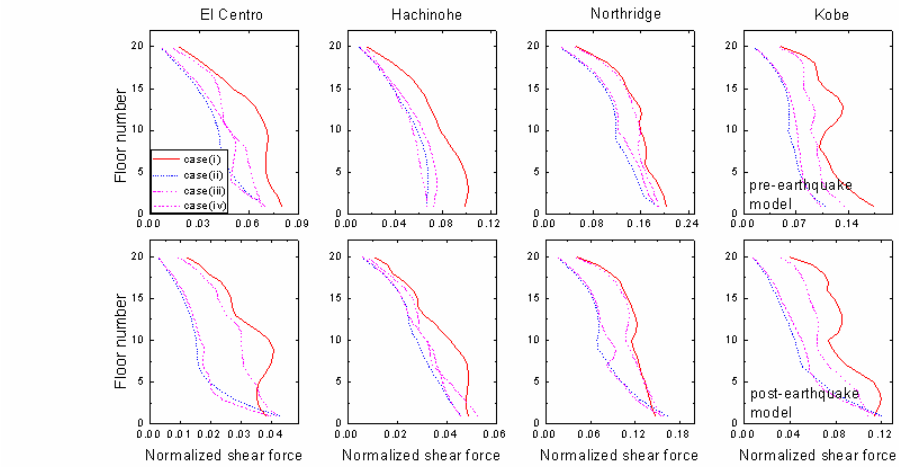

Figure 12. Comparison of story shear forces considering 15 no. of dampers

models of benchmark building. Table 4 and 5 also implies that the values of performance indices of the two models with 15 numbers of SAVFDs are almost as much as of that arrived for the models with dampers installed with all the floors resulting same structural performance with less number of dampers at appropriate locations thereby, reducing cost of dampers.

4. CONCLUSIONS

The behavior of benchmark building installed with SAVFD and passive friction dampers under various earthquake excitations is investigated. The governing equations of motion are formulated in state space form for the benchmark building installed with dampers. The

optimum gain multiplier of the SAVFD for the minimum seismic responses of both the models is studied. Below are the various conclusions drawn from the present numerical study:

1. The SAVFD is effective in reducing the performance criteria J_1 - J_{10} of the benchmark building for both pre- and post-earthquake evaluation models.
2. The optimum gain multiplier for SAVFD for minimum earthquake responses is different for both the models with various earthquakes; however there exists optimum value for the benchmark building with both the evaluation models.
3. Optimum number of dampers at appropriate locations can significantly reduce the earthquake response of both the models almost as much as they are installed on all the floors.
4. The floors with maximum relative displacement/high velocity should be selected as effective damper locations.
5. The seismic response of benchmark building is mitigated by installing with SAVFD; however, performance of SAVFD is as much as that of passive friction damper in respect of displacement reduction.
6. Performance of benchmark building installed with SAVFD against acceleration reduction is much better than with passive friction dampers.

REFERENCES

1. Housner GW, Bergman LA, Caughey TK, Chassiakos AG, Claus RO, Masri SF, Skelton RE, Soong TT, Spencer BF, Yao JTP. Structural control: past, present, and future, *Journal of Engineering Mechanics*, **123**(1997) 897-971.
2. Spencer BF, Nagarajaiah S. State of the art of structural control, *Journal of Structural Engineering, ASCE*, **129**(2003) 845-56.
3. Spencer BF, Christenson RE, Dyke SJ. Next generation benchmark control problem for seismically excited building, *Proceedings of Second World Conference on Structural Control (2WCSC)*, June 28-July 1, Kyoto, Japan, **2**(1998) pp. 1351-1360.
4. Matheu EE, Singh MP, Moreschi LM. Sliding mode control of Los Angeles 20-story benchmark structure, *Second World Conference on Structural Control (2WCSC)*, June 28-July 1, Kyoto, Japan, **2**(1998) pp. 1381-1390.
5. Dyke SJ. Seismic protection of a benchmark building using Magneto-rheological dampers, *Proceedings of the Second World Conference on Structural Control (2WCSC)*, Kyoto, Japan, June 28-July 1, **2**(1998) pp. 1455-1462.
6. Seto K, Matsumoto Y, Kar IN. Design of robust control law to control the vibration of 20 story benchmark building in response to earthquakes, *Proceedings of Second World Conference on Structural Control (2WCSC)*, June 28-July 1, Kyoto, Japan, **2**(1998) pp. 1361-1370.
7. Yoshida O, Dyke SJ. Seismic control of a nonlinear benchmark building using smart dampers, *Journal of Engineering Mechanics*, ASCE, **130**(2004) 386-92.
8. Fukukita A, Saito T, Shiba K. Control effect for 20-story benchmark building using passive or semi-active device, *Journal of Engineering Mechanics*, **130**(2004) 430-6.
9. Chen G, Chen C. Semi-active control of the 20-story benchmark building with

piezoelectric friction dampers, *Journal of Engineering Mechanics*, **130**(2004) 393-400.
10. Kim Y, Langari R, Stefan H. Control of a seismically excited benchmark building using linear matrix inequality-based semi-active nonlinear fuzzy control, *Journal of Structural Engineering, ASCE*, **136**(2010) 1023-26.
11. Aiken ID, Kelly JM. Earthquake simulator testing and analytical studies of two energy-absorbing systems for multi-story structures, Technical Report, UCB/EERC-90/03, University of California, Berkeley, CA, 1990.
12. Hanson RD, Soong TT. Seismic design with supplemental energy dissipation devices, Monograph No. 8, Earthquake Engineering Research Institute, Oakland, 2001.
13. Akbay Z, Aktan HM. Abating earthquake effects on building by active-slip brace devices, *Shock and Vibration*, **2**(1995) 133-42.
14. Kannan S, Uras HM, Aktan HM. Active control of building seismic response by energy dissipation, *Earthquake Engineering & Structural Dynamics*, **24**(1995) 747-59.
15. Inaudi JA. Modulated homogeneous friction: a semi-active damping strategy, *Earthquake Engineering and Structural Dynamics*, **26**(1997) 361-76.
16. Sadek F, Mohraz B. Semi-active control algorithms for structures with variable dampers, *Journal of Engineering Mechanics, ASCE*, **124**(1998) 981-90.
17. Lu LY, Chung LL. Modal control of seismic structure using augmented state matrix, *Earthquake Engineering & Structural Dynamics*, **30**(2001) 237-56.
18. Lu LY. Semi-active modal control for seismic structures with variable friction dampers, *Engineering Structures*, **26**(2004) 437-54.
19. Xu YL, Qu WL, Chen ZH. Control of wind-excited truss tower using semi-active friction damper, *Journal of Structural Engineering, ASCE*, **127**(2001) 861-8.
20. Lu LY. Predictive control of seismic structures with semi-active friction dampers, *Earthquake Engineering & Structural Dynamics*, **33**(2004) 647-68.
21. Lu LY, Chung LL, Lin GL. A general method for semi-active feedback control of variable friction dampers, *Journal of Intelligent Material Systems and Structures*, **15**(2004) 393-412.
22. Kori JG, Jangid RS. Semi-active friction dampers for seismic control of structures, *Smart Structures and Systems*, **4**(2008) 493-515.
23. Patil VB, Jangid RS. Response of wind-excited benchmark building installed with dampers, *The Structural Design of Tall and Special Building*, **20**(2011) 497-514.
24. Naeim Farzad. Performance of Extensively Instrumented Buildings during the January 17, 1994 Northridge Earthquake. JMA Report # 97-7530.68, Report on Contract #1093-557(1997) to the Strong Motion Instrumentation Program, California Division of Mines and Geology, John A. Martin and Associates.
25. Stevenson JD. Structural damping values as a function of dynamic response stress and deformation Levels, *Nuclear Engineering and Design*, **60**(1980) 211-37.
26. Meirovitch L. *Dynamics and Control of Structure*, Wiley, New York, 1990.
27. Ozbulut Osman E, Hurlebaus Stefan. Seismic control of nonlinear benchmark building with a novel re-centering variable friction device, *Proceedings of the Ninth Pacific Conference on Earthquake Engineering Building an Earthquake-Resilient Society*, Paper Number 145, April 14-16, Auckland, New Zealand, 2011.